Performance and Reliability of an Advanced Production GaAs HBT Process Technology

F.M. Yamada*, A.K. Oki, D.C. Streit, B.L. Hikin, E.N. Kaneshiro, M.D. Lammert, L.T. Tran, T.R. Block, P.C. Grossman, J.R. Scarpulla and A.L. Gutierrez-Aitken

TRW Inc.
Electronics & Technology Division
One Space Park D1/1050
Redondo Beach, CA 90278
*Tel: (310) 812-8592, Fax: (310) 813-0418, Email: frank.yamada@trw.com

ABSTRACT

We report on a highly reliable production 1µm GaAs/AlGaAs Heterojunction Bipolar Transistor (HBT) process technology. Our new advanced technology features HBTs with thinner Be-doped base layer, smaller emitter dimensions and higher current density operation than our current production process. Multi-temperature, multi-lot constant stress lifetest projects a median-time-to-failure (MTF) of >10^8 hours for discrete components and for a higher complexity standard evaluation circuit (SEC) implemented in this technology. Discrete HBTs, Schottky diodes, NiCr and CerMet thin-film resistors have been evaluated at the component level. In addition to reliability performance, the DC and RF characteristics of our advanced HBTs are highlighted.

INTRODUCTION

Today's state-of-the-art performance in electronic and communication systems has been achieved largely due to advances in III-V semiconductor technology including GaAs/AlGaAs HBT process technology. GaAs HBTs have been successfully inserted into cutting-edge space/defense systems and high-volume, low-cost commercial applications such as wireless communication [1,2]. The successful insertion of GaAs HBT is due to its inherent advantages in performance over its silicon counterparts, GaAs MESFET and HEMT technologies [3]. In 1999, TRW, RFMD and other major sources were shipping GaAs HBT ICs at an estimated rate of 10 million ICs/month while the forecasted demand for HBTs continues to rise sharply worldwide.

While GaAs HBTs have proven to have favorable price and performance advantages, ensuring a reliable technology is a key factor that establishes TRW's HBT process as a mature technology for providing reliable, high-performance ICs at low cost and high yield to both the space/defense and commercial markets.

This paper briefly describes TRW's advanced production GaAs HBT technology, device characteristics, component and IC reliability. The purpose of component and IC reliability testing was to evaluate and qualify our advanced process technology for space-qualified, Class "K" and commercial IC fabrication. The result advances the state of GaAs HBT technology by demonstrating a reliable, advanced process technology for next-generation system designs.

PROCESS TECHNOLOGY

TRW's advanced 1µm GaAs/AlGaAs HBT production process features Npn GaAs/AlGaAs HBT devices grown on semi-insulating GaAs substrates by solid source molecular beam epitaxy (MBE). The HBT device features include: 800Å $1x10^{19}$ cm^{-3} beryllium doped base layer; 1200Å wide gap emitter layer of $Al_{0.3}Ga_{0.7}As$ with a 300Å $Al_xGa_{1-x}As$ grading on both sides; and 850Å graded InGaAs emitter cap. Silicon is used as the n-type dopant.

This advanced process features HBTs with 1µm minimum emitter width. The emitter and base mesa are formed by wet etch, and boron implantation provides device isolation. AuBe/Pd/Au, AuGe/Ni/Ti/Au and refractory Ti/Pt/Au metalization are used for the base, collector and emitter ohmic contact, respectively.

Other key process features include schottky diodes, PIN diodes, 20Ω/□ and 100Ω/□ NiCr thin film resistors (TFRs), 300Ω/□ CerMet TFR, metal-insulator-metal (MIM) capacitors, multiple interconnect levels, backside ground vias, airbridge crossovers and silicon nitride (SiN) glassivation. In this process, schottky and PIN diodes can be integrated with HBTs without added process complexity due to the common MBE material profile shared between these device structures. All processed wafers are subjected to in-process screening that includes process control monitor testing for process conformance, 48-hour unbiased stabilization bake at 240°C, RF and DC electrical test, and visual inspection.

DEVICE PERFORMANCE & CIRCUIT APPLICATIONS

GaAs HBT is well suited for a wide range of analog, microwave/millimeterwave, digital and mixed-signal functions. The HBT's wide range of applicability is made possible by key device characteristics that are highlighted in Figure 1. Figure 1 also lists some of the more common functions implemented in HBT technology today. These circuit functions are necessary building blocks for modern electronic and communication systems. Most of the functions in Figure 1 have been demonstrated on our advanced production process. For example, one design currently in production is a 5.5GHz frequency synthesizer IC with a very low 18pA/√Hz noise spectral density [4].

Excellent Analog Properties	β>400 @ 1mA Vbe matching (σ≈1mV) Hi Early Voltage (Va≈800V) Ideality Factor (nf≈1.05)
High Frequency-Breakdown Product	Ft ≈ 40 GHz Fmax ≈ 70 GHz BVceo > 15V @ 1μA BVcbo > 22V @ 1μA BVbeo ≈ 7V @ 1μA
High Linearity	Max. IP3/Pdc ≈ 80 @ 12 GHz
Low Noise	1/f corner < 100 kHz NF ≤ 1.3 dB @ L-Band
High Efficiency	PAE ≈ 80% @ L-Band PAE ≈ 65% @ X-Band
Radiation Hard	>500 MRad Total Dose >10^14 Neutron/cm^2

DEVICE CHARACTERISTICS

Integration Capability	Large Scale Integration (LSI) Schottky Diode(Ft>800GHz) PIN Diode (Ft>400GHz) Single Chip μwave & Digital
High Reliability	MTF(125°C) > 10^8 Hours
High Yield	4K HBTs with >30% yield
Low Cost	< $1.00/amplifier

MANUFACTURABILITY

MICROWAVE ICs
Frequency Divider
Frequency Multiplier
High-Intercept Amp
High-Efficiency Power Amp
Low-Noise Amp
Mixer
PSK Modulator
VCO

ANALOG ICs
Four-Quadrant Multiplier
Limiting Amp
Logarithmic Amp
Variable Gain Amp

DIGITAL ICs
Clock Recovery
TTL, CML & ECL Logic
Modulator Driver
Mux & Demux

MIXED-SIGNAL ICs
A to D Converter (ADC)
D to A Converter (DAC)
Frequency Synthesizer

ELECTRO-OPTIC ICs
EO Modulator Driver
Laser Driver
Transimpedance Amp

CIRCUIT FUNCTIONS

Figure 1. Key device characteristics and high manufacturability of TRW's advance production HBT technology leads to a wide range of circuit applications.

RELIABILITY

Our approach to evaluating the overall reliability of a new technology is to perform reliability tests at both the component and the IC level. Long-term reliability assessment is determined by means of multi-temperature, multi-lot constant stress lifetests where component and IC aging are accelerated at elevated temperatures under DC bias. Constant stress lifetest is an effective methodology for semiconductor reliability testing and can be used to determine factors such as failure distribution, median-time-to-failure (MTF) and activation energy (Ea) based on the Arrhenius life-temperature relationship. These factors allow the user to estimate device or IC lifetime and failure rate at a user-specified temperature.

In this paper we report on five discrete components and one SEC IC. The reliability result referenced to 125°C junction or film temperature is summarized in Table I [5]. Table I also list the current density (Jc) stress condition and failure criterion for each component. The Δ failure criterion is referenced to pre-lifetest values. All components and the SEC exhibited a well-behaved log-normal failure distribution with a low, temperature-insensitive log standard deviation (σ). The low σ is indicative of a very well controlled process. Evaluation of each component is described in the following subsections.

A. NiCr TFRs.

NiCr TFRs of different film thickness for 100Ω/□ and 20Ω/□ nominal values was lifetested independently. 100Ω/□ TFR at 3000 kA/cm^2 operation has a projected MTF of 3.6x10^8 hours at 125°C film temperature. A 3% change in resistance from pre-stress level was established as the critical failure criterion. Similarly, the 20Ω/□ TFR at 2000 kA/cm^2 operation has a projected MTF of 4.8x10^8 hours where failure is defined as a 1.5% change in resistance from pre-stress level. The log-normal failure distribution and Arrhenius life-temperature model for 100Ω/□ and 20Ω/□ TFRs is plotted in Figure 2 and 3, respectively.

NiCr TFR was observed to be very robust where the nominal resistance increases by only 3% after being stressed for 4700 hours under 3000 kA/cm^2 at 266°C. The very low σ (0.2-0.3) translates to excellent tracking between TFRs over the IC's lifetime. TFR matching and tracking can be critical in high-precision circuits such as ADCs. In addition, a recent lifetest has concluded that NiCr TFRs can operate at current densities much higher then 3000 kA/cm^2 while maintaining a slow degradation rate and tight dispersion pattern.

Both compositionally equivalent TFR components exhibit an Ea of 1.5eV indicating a common degradation mechanism. The dominant failure mechanism is presumed to be contact degradation. Electromigration is also a possible failure mechanism however the measured Ea of 1.5eV is inconsistent with previously reported Ea of 0.8-1.1 eV for electromigration in NiCr film [6,7]. Due to the small ΔR that could be induced during the lifetest, only a limited failure analysis was performed on the NiCr TFRs.

B. CerMet TFRs.

High-precision, laser-trimmable CerMet TFRs was introduced into our advanced process. 300Ω/□ CerMet TFR under 230 kA/cm^2 operation has a projected MTF of 5.4x10^8 hours and a very low σ of 0.3. A 10% change in resistance from pre-stress level was established as the critical failure criterion. The log-normal failure distribution and Arrhenius model is plotted in Figure 4. The dominant failure mechanism is believed to be CerMet annealing characterized by a 1.9eV Ea.

TABLE I. LIFETEST SUMMARY OF COMPONENTS AND SEC FROM THE 1μm GaAs HBT TECHNOLOGY

Component or IC	Jc, max (kA/cm^2)	Failure Criterion	Log-Sigma σ	Ea (eV)	MTF@125°C (Hours)	Failure Rate h(t≤10yrs@125°C) (FITs)	Dominant Failure Mechanism
NiCr TFR (100Ω/□)	3000	|ΔR/Ro| >0.03	0.2	1.5	3.6x10^8	<< 10^{-6}	Presumably Contact Degradation
NiCr TFR (20Ω/□)	2000	|ΔR/Ro| >0.015	0.3	1.5	4.8x10^8	<< 10^{-6}	Presumably Contact Degradation
CerMet TFR	230	|ΔR/Ro| >0.10	0.3	1.9	5.4x10^8	<< 10^{-6}	CerMet Annealing
Schottky Diode	23	|ΔVd(10mA)| >40mV	0.6	2.4	2.9x10^{11}	<< 10^{-6}	Ohmic Degradation
Discrete HBT	35.3	Δβ/βo < -0.10	0.8	2.1	2.0x10^9	<< 10^{-6}	Substitutional Be Migration
SDLA SEC	25	|ΔVout| >90mV	0.6	1.9	5.1x10^8	<< 10^{-6}	Presumably Substitutional Be Migration

C. Schottky Diodes.

$10x10\mu m^2$ Schottky diodes under 23 kA/cm^2 operation has a projected MTF of $2.9x10^{11}$ hours at 125°C junction temperature. A shift of >40mV in diode voltage at 10mA diode current from pre-stress level was established as the critical failure criterion. The log-normal failure distribution and Arrhenius model is plotted in Figure 5. Dominant failure mechanism is ohmic contact degradation.

D. Discrete HBTs.

Discrete HBTs grown by MBE have demonstrated $2x10^9$ hours MTF at 125°C junction temperature where a 10% degradation in device current gain (ß) from its pre-stress level was established as the critical failure criterion. The log-normal failure distribution and Arrhenius life-temperature relationship is plotted in Figure 6. Failure distribution follows a classical log-normal behavior with a measured σ of 0.8. Based on the log-normal probability distribution and density function, an instantaneous failure rate of $<<10^{-6}$ FITs (failures per billion device hours) for a 10-year mission at 125°C junction temperature has been calculated.

Failure mechanism in Be-doped HBTs is substitutional Be migration from base to graded AlGaAs emitter during biased operation. The p-type dopant migration compromises the base-emitter heterojunction leading to a decrease in ß and increase in turn-on voltage. This degradation has been observed in the device Gummel plot. ß degradation with Ea=2.1eV is consistent with independent reports of Ea≈1.6-2.1eV for diffusion coefficient of Be in GaAs [8-10].

E. Standard Evaluation Circuit (SEC).

At the IC level, proper selection of a SEC and its failure criteria are essential to demonstrate and fully evaluate the reliability of a technology. The Successive Detection Logarithmic Amplifier (SDLA) is currently being used as a SEC based on its difficult analog requirements, its circuit complexity, its logging function's high sensitivity to both RF and DC drift in the HBTs and other passive components. The SDLA consist of 216 HBTs, 261 TFRs, 23 MIMs and 9 backside ground vias. The SDLA implemented in our advanced process is nearly identical to a SDLA design that has been reported previously [11]. The only difference is the substitution of 1µm HBTs and CerMet TFRs.

For this lifetest the log video output, Vout, was selected as the performance parameter to monitor since the video signal path provides the most complex and sensitive path in the SDLA. For reliability assessment, $|\Delta Vout| > 90mV$ at 0.475GHz IF and -30dBm input power was established as the failure criterion. This criterion is equivalent to a 0.5dB input referred gain change for every 10dB of RF gain. For comparison, typical MESFET and HEMT reliability testing uses a failure criterion of 1.0 dB gain degradation for every 10-12dB of RF gain of a MMIC amplifier.

The SEC's failure distribution is plotted in Figure 7 and exhibits a well-behaved log-normal distribution with σ=0.6. The Arrhenius model adjusted for device junction temperature rise is also plotted in Figure 7. The SEC operating at ≈25 kA/cm^2 projects a MTF of $5.1x10^8$ hours at 125°C junction temperature with Ea=1.9eV.

The exact failure mechanism for the SEC could not be determined directly due to circuit complexity. However, the SEC failure mechanism is presumed to be the same substitutional Be migration observed in discrete HBTs. The SEC's 1.9eV Ea is within measurement accuracy to the discrete HBT's 2.1eV Ea and consistent with properties of Be diffusion [8-10]. In addition, SPICE analysis modeling Be migration shows good agreement between simulated and measured SEC transfer function.

SUMMARY

The device characteristics and performance of GaAs HBTs make them suitable for a wide range of analog, microwave/millimeterwave, digital and mixed-signal applications. Our advanced production 1µm GaAs HBT process featuring HBTs with thinner Be-doped base layer, smaller emitter dimensions and higher Jc operation is providing a technological advancement for next-generation systems.

The MBE-grown GaAs HBT device is shown to be a fundamentally reliable device structure. Passive components implemented in our advanced technology also exhibits excellent reliability. The reliability of the overall HBT process technology is demonstrated by lifetesting of a monolithic SEC IC with a resulting MTF of $5.1x10^8$ hours at 125°C junction temperature with an associated activation energy of 1.9eV.

Our advanced HBT technology have been evaluated and space-qualified for Class "K" IC fabrication. Extensive reliability testing has repeatedly demonstrated excellent and consistent reliability performance that is more than capable of meeting today's space/defense and commercial reliability requirements for microelectronics.

REFERENCES

[1] Meyer, M., Compound Semiconductor, pp. 30-39, May/June 1997.

[2] Bechtel, G., IEEE GaAs IC Symp. Tech. Digest, pp. 7-9, October 1999.

[3] Kim, M.E., et al., IEEE Microwave Theory and Techniques **37**, pp. 1286-1303, September 1989.

[4] Diorio, C., et al., IEEE Journal of Solid-State Circuits, Vol.33, No. 9, pp. 1306-1312, September 1998.

[5] Yamada, F.M., et al., GaAs IC Reliability Workshop, October, 1999

[6] Satake, T., Appl. Phys. Lett., Vol.23, No.9, pp. 496-498, Nov. 1973.

[7] Fraser, A., et al., IEEE GaAs IC Symp. Tech. Digest, pp. 161-164, October 1985.

[8] Uematsu, M., et. al., Appl. Phys. Lett., Vol. 58 No. 18, pp. 2015-2017, May 1991.

[9] Schubert, E.F., et. al., J. Appl. Phys. Vol. 67 No. 4, pp. 1969-1979, February 1990.

[10] Tejwani, M.J., et. al., Appl. Phys. Lett., Vol. 53 No. 24, pp. 2411-2413, December 1988.

[11] Yamada, F.M., et al., IEEE GaAs IC Symposium Tech. Digest, pp. 271-274, October 1994.

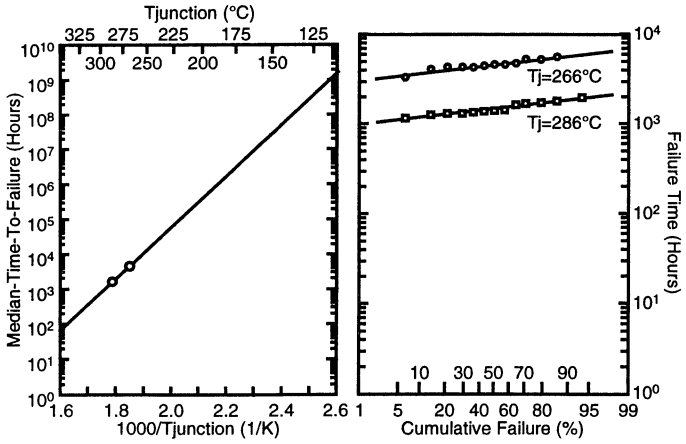

Figure 2. Arrhenius life-temperature model (left) and log-normal failure distribution (right) for 100Ω/□ NiCr TFRs stressed at 3000kA/cm^2. The MTF at 125°C is 3.6x10^8 hours with an associated Ea of 1.5eV. Failure distribution exhibits a σ of 0.2. Tj is the film temperature.

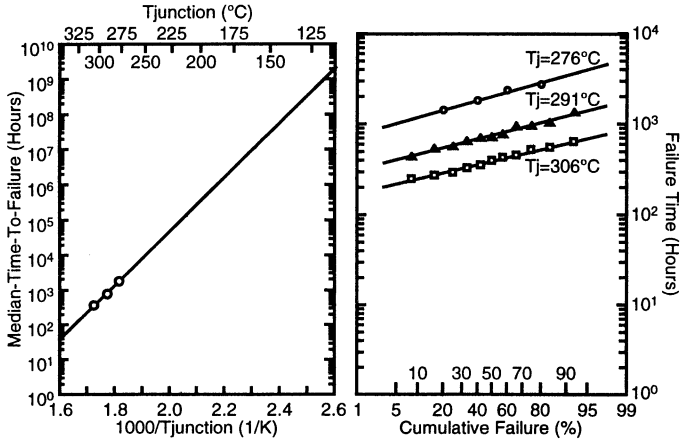

Figure 3. Arrhenius life-temperature model (left) and log-normal failure distribution (right) for 20Ω/□ NiCr TFRs stressed at 2000kA/cm^2. The MTF at 125°C is 4.8x10^8 hours with an associated Ea of 1.5eV. Failure distribution exhibits a σ of 0.3. Tj is the film temperature.

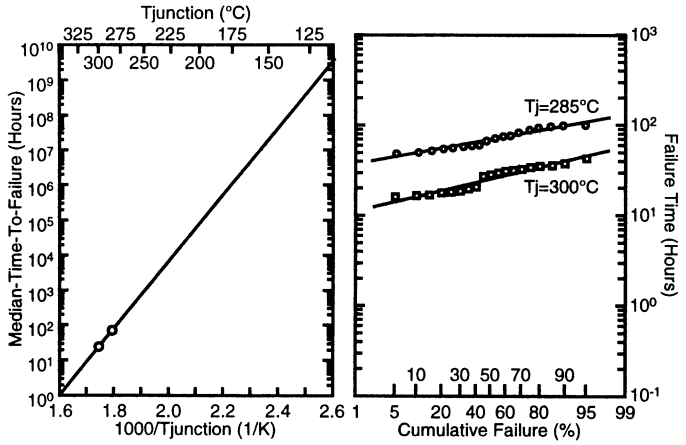

Figure 4. Arrhenius life-temperature model (left) and log-normal failure distribution (right) for 300Ω/□ CerMet TFRs stressed at 230kA/cm^2. The MTF at 125°C is 5.4x10^8 hours with an associated Ea of 1.9eV. Failure distribution exhibits a σ of 0.3. Tj is the film temperature.

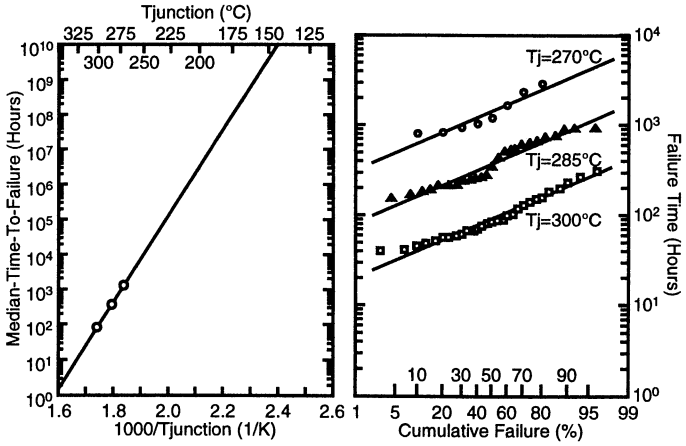

Figure 5. Arrhenius life-temperature model (left) and log-normal failure distribution (right) for discrete Schottky diodes stressed at 23kA/cm^2. The MTF at 125°C is 2.9x10^{11} hours with an associated Ea of 2.4eV. Failure distribution exhibits a σ of 0.6. Tj is the junction temperature.

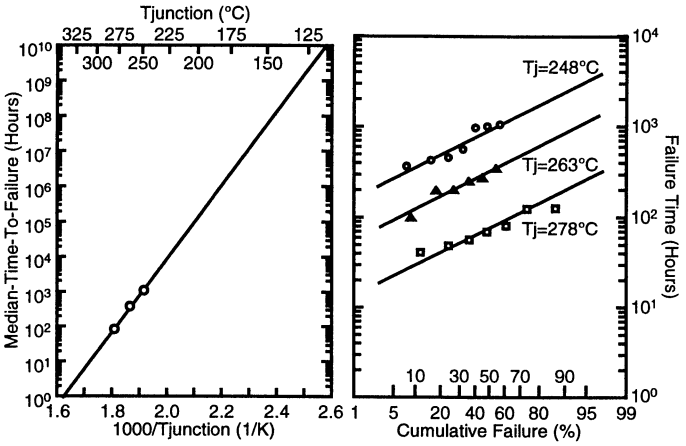

Figure 6. Arrhenius life-temperature model (left) and log-normal failure distribution (right) for discrete 1μm GaAs HBTs stressed at 35.3kA/cm^2. The MTF at 125°C is 2.0x10^9 hours with an associated Ea of 2.1eV. Failure distribution exhibits a σ of 0.8. Tj is the junction temperature.

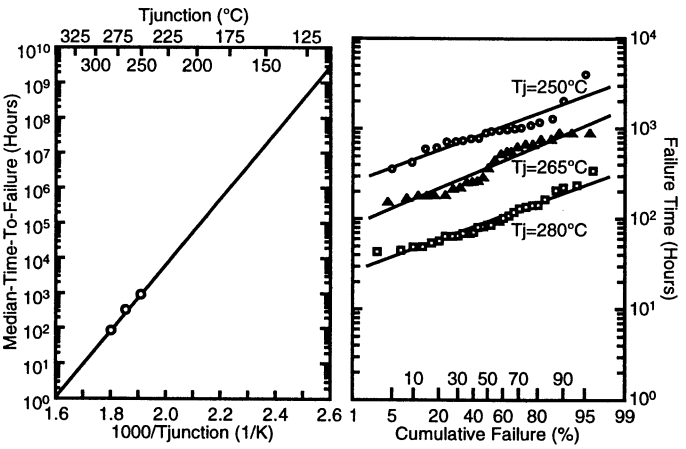

Figure 7. Arrhenius life-temperature model (left) and log-normal failure distribution (right) for SDLA SECs stressed at 25kA/cm^2. The MTF at 125°C is 5.1x10^8 hours with an associated Ea of 1.9eV. Failure distribution exhibits a σ of 0.6. Tj is the junction temperature of the hottest HBT.